RESEARCH ARTICLE

Synthesis of Chromenes using functionalized SBA-15

Hossein Shahbazi-Alavi[1,*], Atefeh Bakhtiari[2], Homayoun Gholamzadeh[3], Javad Safaei-Ghomi[2]

[1] Young Researchers and Elite Club, Kashan Branch, Islamic Azad University, Kashan, Iran.

[2] Department of Organic Chemistry, Faculty of Chemistry, University of Kashan, Iran.

[3] Department of Polymer Engineering, Qom University of Technology, Iran.

ARTICLE INFO

Article History:
Received 2021-04-15
Accepted 2022-11-12
Published 2022-03-01

Keywords:
Nanocatalyst
SBA-15
Nanoanalysis
Chromene

ABSTRACT

Functionalized SBA-15 (Immobilization of Pd on the modified SBA-15) has been utilized as an efficient catalyst for the preparation of chromenes by multi-component reactions of aromatic aldehydes, malononitrile and 4-hydroxycoumarin under reflux in ethanol. The catalyst has been characterized by X-ray diffraction spectroscopy (XRD), Field emission scanning electron microscopy (FE-SEM), Transmission electron microscopy (TEM), Energy-dispersive X-ray spectroscopy (EDX), X-Ray photoelectron spectroscopy (XPS), Fourier-transform infrared spectroscopy (FT-IR), N_2 adsorption analysis, Temperature Programmed Desorption (TPD), and Differential thermal analysis (TGA-DTA). The advantages of this method include the reusability of the catalyst, low catalyst loading, excellent yields in short reaction times and easy separation of products, with no recrystallization required.

How to cite this article
Shahbazi-Alavi H., Bakhtiari A., Gholamzadeh H., Safaei-Ghomi J . Synthesis of Chromenes using functionalized SBA-15. J. Nanoanalysis., 2022; 9(1): 49-61. DOI: 10.22034/jna.2022.1928076.1252.

INTRODUCTION

Chromenes possess many biological properties containing activities against cancer [1], pathogenic microbes [2] viruses [3] inflammation [4] diabetes [5], and Alzheimer's disease [6]. Some chromene drugs are notable for their high bioavailabilities and prolonged duration of effect [7]. Therefore, the synthesis of organic compounds continues to be a notable challenge [8-12]. A number of ways have been developed for the preparation of chromenes using lipase [13], *p*-TSA [14], Et_3N [15], Zn[L-proline]$_2$ [16], $[Et_3NH][HSO_4]$ [17], DBU [18], $Cu(OTf)_2$ [19], triethylbenzylammonium chloride [20], [bmim]OH [21,22], and sodium malonate [23], While the development of each of these methods has contributed to moving the field forward, some also suffer from such drawbacks as prolonged reaction times, complicated work-up, low yield, or hazardous reaction conditions. Therefore, to avoid these drawbacks, finding of an effective way to prepare chromenes is still favored. Microporous materials with regular-pore frameworks are a good choice for immobilizing the ligands [24]. An improved understanding of the efficiency of ordered mesoporous silica could be obtained by evaluating their potential application in drug delivery, separation, gas storage, catalysis, and biomolecules [25]. SBA-15 was employed due to its properties such as large pore volume, uniform-sized pores, high special surface area and thermal and hydrothermal stability [26]. The anchoring of a wide range of organic functional groups to the pore surface of SBA-15 improves the catalytic ability [27]. A stable attachment of ligand could be reached by post-synthetically of the available ligand precursors to SBA-15 [28]. Herein, we report the use of functionalized SBA-15 as an effective catalyst for the preparation of chromenes by multi-component reactions of aromatic aldehydes, malononitrile and 4-hydroxycoumarin under reflux in ethanol (Scheme 1). Ideally, utilizing environmental and green catalysts which can be

* Corresponding Author Email: *hosseinshahbazi99@yahoo.com*

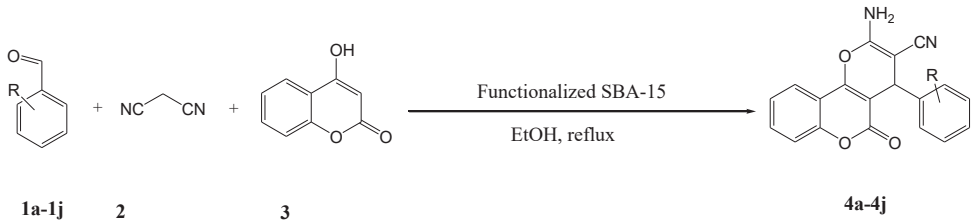

1a-1j **2** **3** **4a-4j**

Scheme 1. Synthesis of chromenes catalyzed by Functionalized SBA-15.

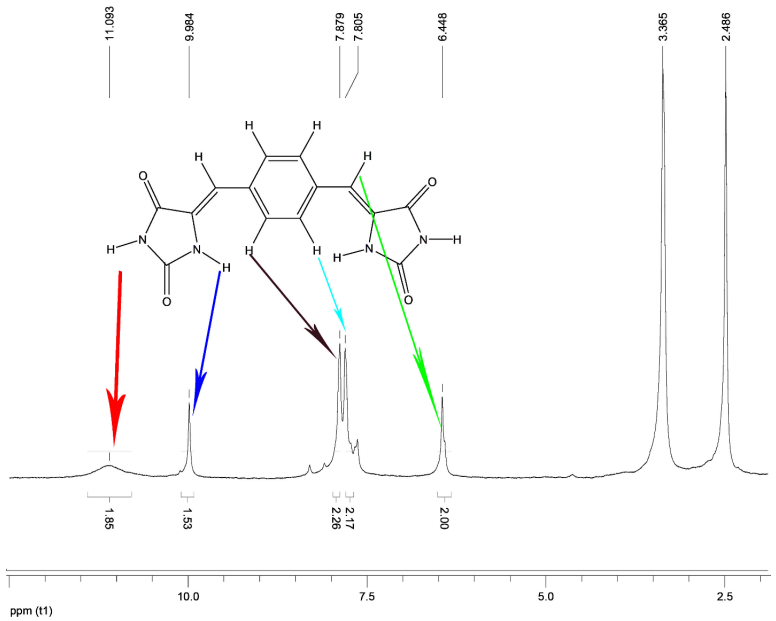

Fig. 1. ^{1}H NMR of ligand (imidazolidone) DMSO.

easily recycled at the end of reactions has obtained great attention in recent years. Nanostructures have emerged as a suitable group of heterogeneous catalysts owing to their numerous applications in synthesis and catalysis. Since, these nanostructures are often recovered simply by easy workup, which prevents contamination of products, they may be considered as a promising safe and reusable catalysts as well as greener compared to traditional catalysts. We found that functionalized SBA-15 produces our desired compounds in high yields with excellent recovery and simple work-up procedure. In addition, functionalized SBA-15 has a good recycling properties and this advantage is important from an economic point of view.

EXPERIMENTAL SECTION

Chemicals and apparatus

NMR spectra were recorded on Bruker Avance-400 MHz spectrometers in the presence of tetramethylsilane as an internal standard. The IR spectra were recorded on FT-IR Magna 550 apparatus using KBr plates. Melting points were determined on Electro thermal 9200. The elemental analyses (C, H, N) were obtained from a Carlo ERBA Model EA 1108 analyzer. The XRD patterns were evaluated using an X-ray diffractometer (PHILIPS, PW 1510, Netherlands) with Cu-Ka radiation (λ = 0.154056 nm) in the range 2θ= 0–10°. The TGA-DTA analyses were performed using a Bahr STA-503 instrument in air at a heating rate of 10 °C min^{-1}. The N_2 adsorption analysis was recorded at -196 °C using an automated gas adsorption analyzer (BEL SORP mini II) and the pore diameter was calculated from the adsorption branch of the isotherm by using the BJH model. The FESEM analysis of the nanostructures was carried out using a Model FE-SEM. The TEM imaging analysis was performed using a Philips EM208 transmission electron microscope with an

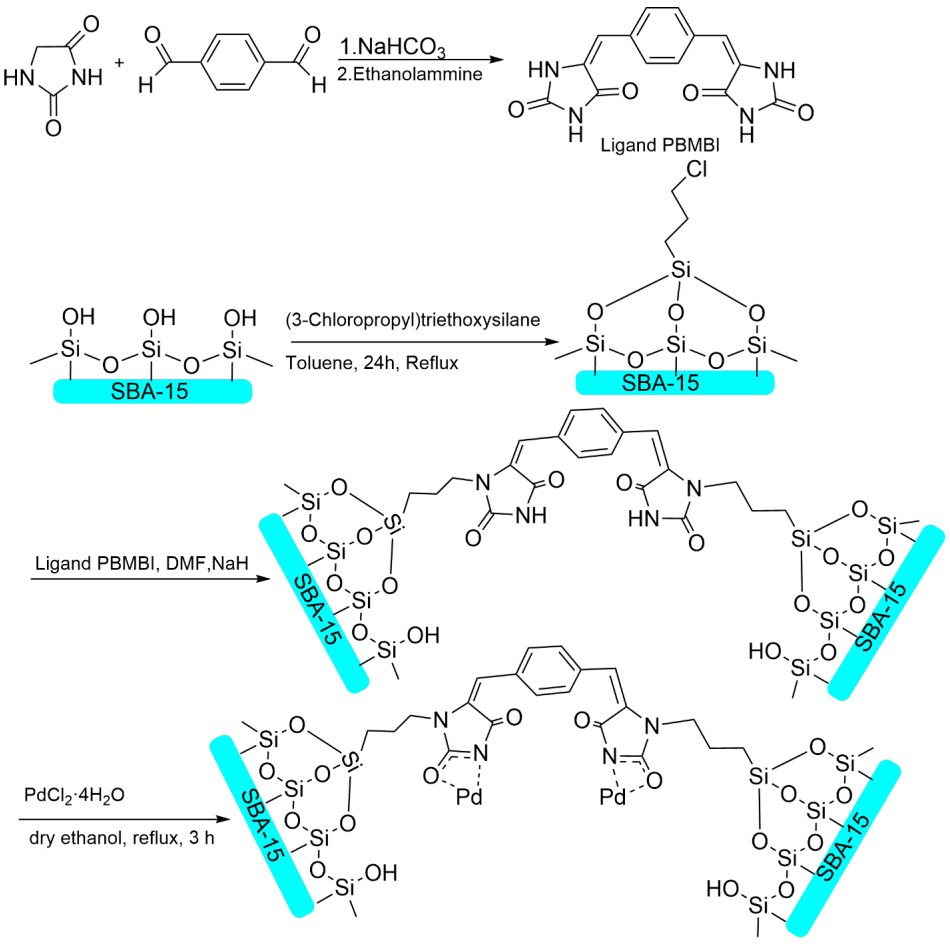

Scheme 2. Different steps for synthesis of Immobilization of Pd on the modified SBA-15 (Pd@modified SBA-15).

accelerating voltage of 200 kV. The EDX analysis of the nanostructures was carried out using a Sigma ZEISS, Oxford Instruments Field Emission. In the NH3-TPD experiments, samples were pretreated at 573 K for 1 h. After that, NH_3 was adsorbed at 373 K for 0.5 h. Then, physically adsorbed ammonia was removed with a pure nitrogen flow at 373 K. XPS spectra were recorded using a ESCA System 100 spectrometer (VSW Scientific Instruments, Manchester).

Preparation of Ligand (imidazolidone)

In a 50 ml round-bottom flask, 4 mmol of hydantoin was dissolved in 4 mL water. Then an amount of saturated sodium hydrogen carbonate solution was added and the pH of the reaction mixture was maintained at 7.0. After that, ethanolamine (0.36 mL) was added, and the solution was warmed up gradually to 90 ˚C. A solution of terephthaldehyde (4 mmol) in 4 mL of ethanol was added dropwise. Then the mixture was continuously stirred for 48 h at 120 ˚C and kept under reflux. A precipitate was formed by cooling in an ice-salt bath at about 0 ˚C. It was filtered and washed with H_2O/EtOH 5:1. The structure of ligand (imidazolidone) was confirmed by ^{1}H NMR and FT-IR spectrum presented in Figs. 1 and 5, respectively.

Preparation of SBA-15 nanostructure

The hexagonal pore structure of SBA-15 has been produced using pluronic 123 triblock copolymers (EO20–PO70–EO20) by the procedure as reported in the previous paper [29].

Preparation of 3-chloropropyltriethoxysilane attached to SBA-15 (chlorinated-SBA-15)

In a 50 mL round-bottom flask, 3 mmol of

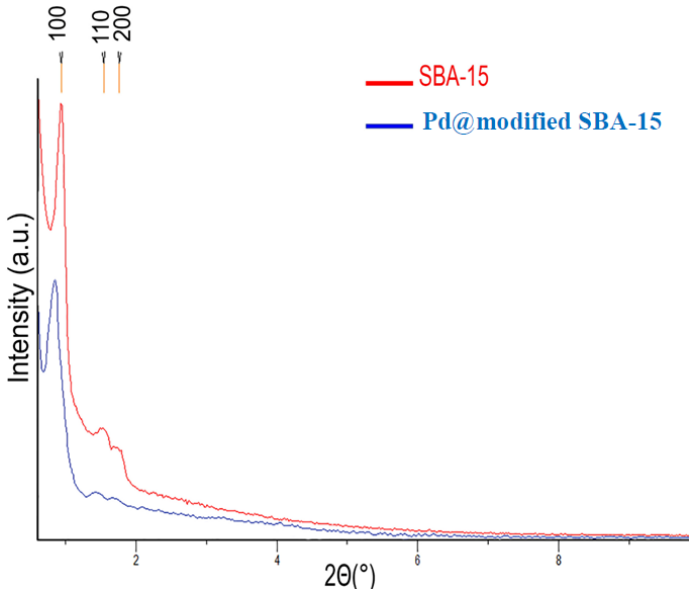

Fig. 2. The XRD pattern of SBA-15 and Pd@modified SBA-15.

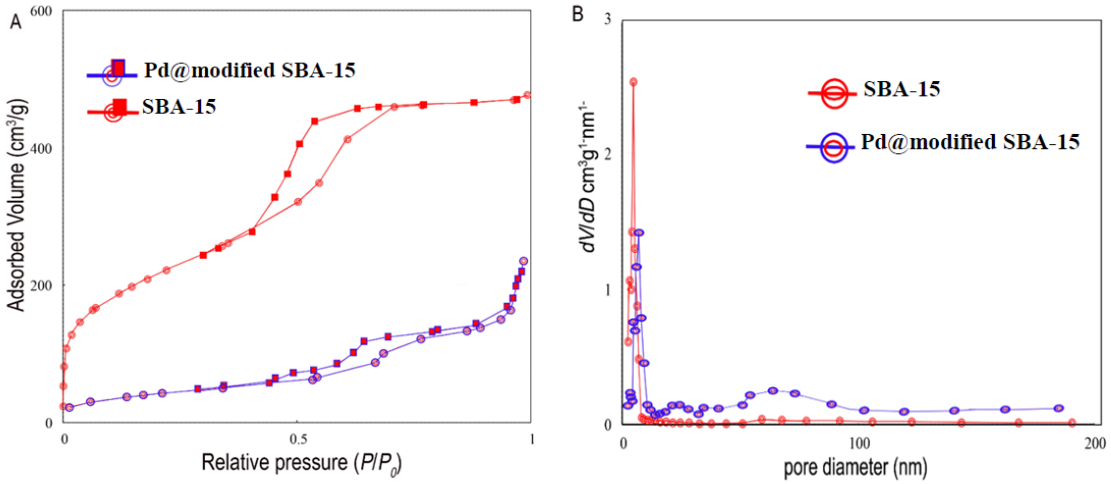

Fig. 3. N_2 adsorption-desorption isotherms and pore size distributions of SBA-15, Pd@modified SBA-15.

3-chloropropyltriethoxysilane and 1 g of calcined SBA-15 were suspended in dry toluene and refluxed at 80 ˚C under an inert atmosphere for 24 h. Then, the solid was filtered and washed successively with ethanol. Finally, the white powder was dried under vacuum at 70 ˚C for 8 h to generate the 3-chloropropyltriethoxysilane attached to SBA-15 (Cl-modified SBA-15).

Preparation of modified SBA-15 (Immobilization of ligand (imidazolidone) to chlorinated-SBA-15)

The solution of ligand (imidazolidone) (2 mmol) in dimethylformamide (10 mL) was added to 60% suspension of sodium hydride. The resulting mixture was stirred for 60 minutes. Then chloro-modified SBA-15 (4.5 g, 26.3 mmol) was added to the reaction mixture. The solution was warmed up gradually to 80 ˚C and stirred for 18 h. The reaction was quenched with 1 N HCl (20 mL, 20 mmol) and the precipitated solid was collected by centrifugation, and then a pure product was obtained by washing with EtOH to produce modified SBA-15 (Immobilization of ligand (imidazolidone) to chlorinated-SBA-15).

Table 1. Structural and Textural Parameters of SBA-15 and Pd@modified SBA-15.

Entry	Sample	*S* BET[a] [m^2 g^{-1}]	D_P[b] [nm]	V_P[c] [cm^3 g^{-1}]
1	SBA-15	758.68	9.40	0.7378
2	Pd/PBMBI-SBA-15	161.89	7.59	0.3587

[a] *S* BET = surface area. [b] *D*p = average pore width. [c] *V*p = total pore volume.

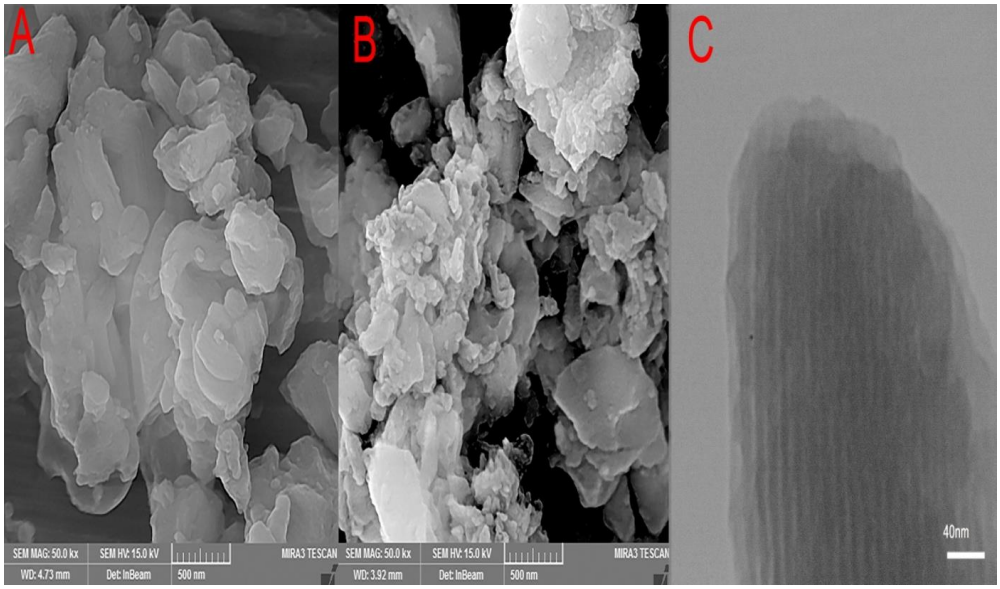

Fig. 4. SEM images of (A) SBA-15 and (B) Pd@modified SBA-15 (C) TEM image of Pd@modified SBA-15.

Preparation of Immobilization of Pd on the modified SBA-15 (catalyst)

To a suspension of modified SBA-15 (1 g) in dry ethanol (20 mL), 0.1 g of $PdCl_2$ was added and the solution was refluxed for 3 h. The yellow light solid was separated by centrifuging and it was dried. Unreacted palladium from the surface was removed using Soxhlet extracted with acetone.

Synthesis of chromenes

A mixture of aldehyde (1 mmol), malononitrile (1 mmol), 4-hydroxycoumarin (1 mmol) and 6 mg functionalized SBA-15 (catalyst) was stirred in 5 mL ethanol at reflux. The reaction was monitored by TLC (*n*-hexane/ethyl acetate 6:4). After completion of the reaction, the catalyst was insoluble in hot ethanol and it could therefore be removed and recycled by a simple filtration while the reaction mixture was still hot. The catalyst was washed with a little hot ethanol, dried in an oven at 80 °C for 6 hours, and then reused for the next run as indicated above for the model reaction. Water was added to the filtrate, and the resulting precipitate was collected by filtration and washed with water. No further purification was needed. The characterization data of the compounds (4a, 4b and 4c) are given below.

2-Amino-4,5-dihydro-4-(4-nitrophenyl)-5-oxopyrano[3,2-c]chromene-3-carbonitrile (4a)

Pale yellow solid, mp 260-262 °C; IR (KBr) (ν_{max}/cm^{-1}): 3479, 3429, 3070, 2195, 1725, 1504, 1350; ^{1}H NMR (400 MHz, DMSO-d_6): δ (ppm) 4.66 (1H, CH), 7.45 (1H, d, *J* = 8.3 Hz, HAr), 7.50 (1H, t, *J* = 7.7 Hz, HAr), 7.59 (2H, br s, NH_2), 7.60 (2H, d, *J* = 8.0 Hz, HAr), 7.75 (1H, t, *J* = 7.8 Hz, HAr), 7.91 (1H, d, *J* = 7.8 Hz, HAr), 8.17 (2H, d, *J* = 8.3 Hz, HAr); ^{13}C NMR (100 MHz, DMSO-d_6): δ (ppm) 38.52, 57.62, 103.66, 113.75, 117.48, 119.79, 123.42, 124.54, 125.55, 130.06, 133.98, 147.47, 151.60, 153.12, 154.82, 158.94, 160.43. *Anal.* Calcd. for $C_{19}H_{11}N_3O_5$: C, 63.16; H, 3.07; N, 11.63. Found: C, 63.05; H, 3.02; N, 11.53.

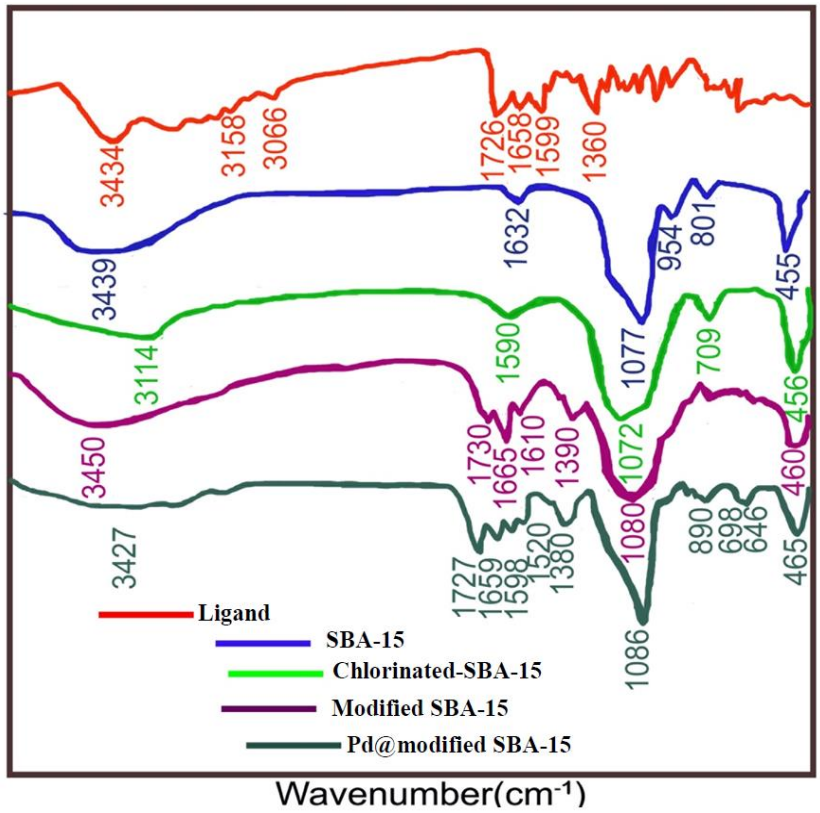

Fig. 5. FT-IR spectra of ligand, SBA-15, chlorinated-SBA-15, modified SBA-15, Pd@modified SBA-15.

2-Amino-4,5-dihydro-4-(4-bromophenyl)-5-oxopyrano[3,2-c]chromene-3-carbonitrile (4b)

Yellow solid, mp 255-257 °C; IR (KBr) (ν_{max}/ cm^{-1}): 3388, 3311, 3187, 2192, 1710, 1606, 1376; ^{1}H NMR (400 MHz, DMSO-d_6): δ (ppm) 4.47 (1H, CH), 7.28-7.30 (2H, CH, d, J = 8 Hz), 7.34-7.36 (2H, CH, d, J = 8 Hz), 7.40-7.50 (4H, CH and NH_2), 7.70-7.74 (1H, CH, t, J = 8 Hz), 7.87-7.89 (1H, CH, d, J = 8 Hz); ^{13}C NMR (100 MHz, DMSO-d_6): δ (ppm) 38.25, 57.45, 103.60, 113.73, 117.42, 119.75, 120.14, 123.40, 124.62, 125.44, 130.07, 133.95, 147.44, 153.14, 154.75, 158.85, 160.12. *Anal.* Calcd. for $C_{19}H_{11}BrN_2O_3$: C, 57.74; H, 2.81; N, 7.09. Found: C, 57.63; H, 2.78; N, 7.03.

2-Amino-4,5-dihydro-4-(4-methoxyphenyl)-5-oxopyrano[3,2-c]chromene-3-carbonitrile (4c)

White solid, mp 242-244 °C; IR (KBr) (ν_{max}/ cm^{-1}): 3372, 3288, 3184, 2192, 1718, 1380; ^{1}H NMR (400 MHz, DMSO-d_6): δ (ppm) 3.70 (OCH_3, 3H), 4.38 (1H, CH), 6.84-6.86 (2H, CH, d, J = 8 Hz), 7.14-7.17 (m, 2H, CH), 7.35-7.49 (m, 4H, CH and NH_2), 7.67-7.69 (1H, t, J = 8 Hz), 7.87-7.89 (m, 1H); ^{13}C NMR (100 MHz, DMSO-d_6): δ (ppm) 36.63, 55.49, 58.71, 104.73, 113.45, 114.30, 116.97, 119.70, 122.89, 125.07, 129.19, 133.28, 135.83, 152.53, 153.50, 158.37, 158.79, 159.95. *Anal.* Calcd. for $C_{20}H_{14}N_2O_4$: C, 69.36; H, 4.07; N, 8.09. Found: C, 69.21; H, 4.03; N, 8.02.

RESULTS AND DISCUSSION

Scheme 2 shows the preparation of the Immobilization of Pd on the modified SBA-15 (catalyst).

The structure of ligand (imidazolidone) was confirmed by ^{1}H NMR and FT-IR spectrum presented in Figs. 1 and 5, respectively.

The effect of modification of the structural framework of SBA-15 is monitored by a small-angle X-ray diffraction method (Fig. 2). A significant degree of long-range ordering of the structure has been determined by an intense diffraction peak (1 0 0). Two secondary high order peaks with lower intensities corresponding to (1 1 0) and (2 0 0) approve 2D-hexagonal planes of the mesoporous [30]. On modification with ligand and metal, the intensities of the peaks are decreased that can be related to the occurrence of silylation inside the

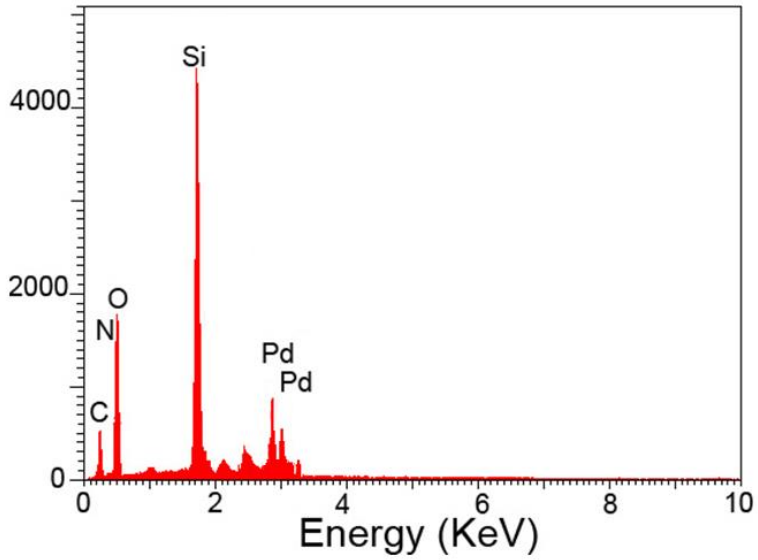

Fig. 6. EDX spectrum of Pd@modified SBA-15.

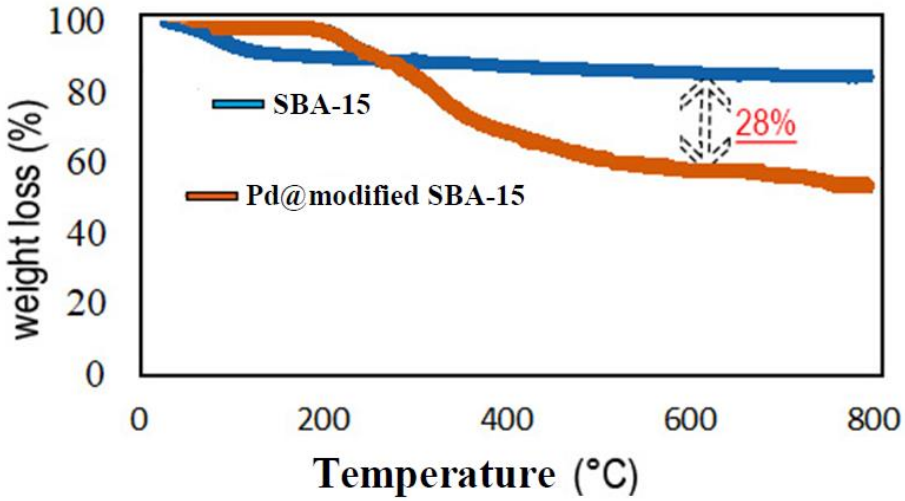

Fig. 7. TGA and DTA curves of SBA-15 and Pd@modified SBA-15.

mesopores of SBA-15. The presence of similar peaks for Pd@modified SBA-15 indicates that the structural ordering of SBA-15 is not diminished during the silylation procedure. The 2D-hexagonal structure of SBA-15 is also preserved regardless of the ligand and metal loading.

The porous structure of SBA-15 and Pd@ modified SBA-15 are analyzed by N_2 sorption isotherms and pore size distributions (Fig. 3). Type IV adsorption-desorption isotherm with an H1 hysteresis loop is observed in both of them, which can be characterized as mesoporous solids [31]. The isotherm of Pd@modified SBA-15 indicates a lower nitrogen uptake, related to a diminution in pore volume and the specific surface area (Table 1). The height of the capillary condensation step slightly reduces due to pore blocking effect by changing in pore size distribution. Indeed, less uniformity of the mesopore size distribution is visible in functionalized SBA-15.

The FESEM of the SBA-15 and Pd@modified SBA-15 show a structural integrity morphology (Fig. 4 a,b). The integrity of the porous structure of SBA-15 is preserved after loading Palladium and ligand. 2D Hexagonal network of the Pd@modified SBA-15 is determined by the TEM image that

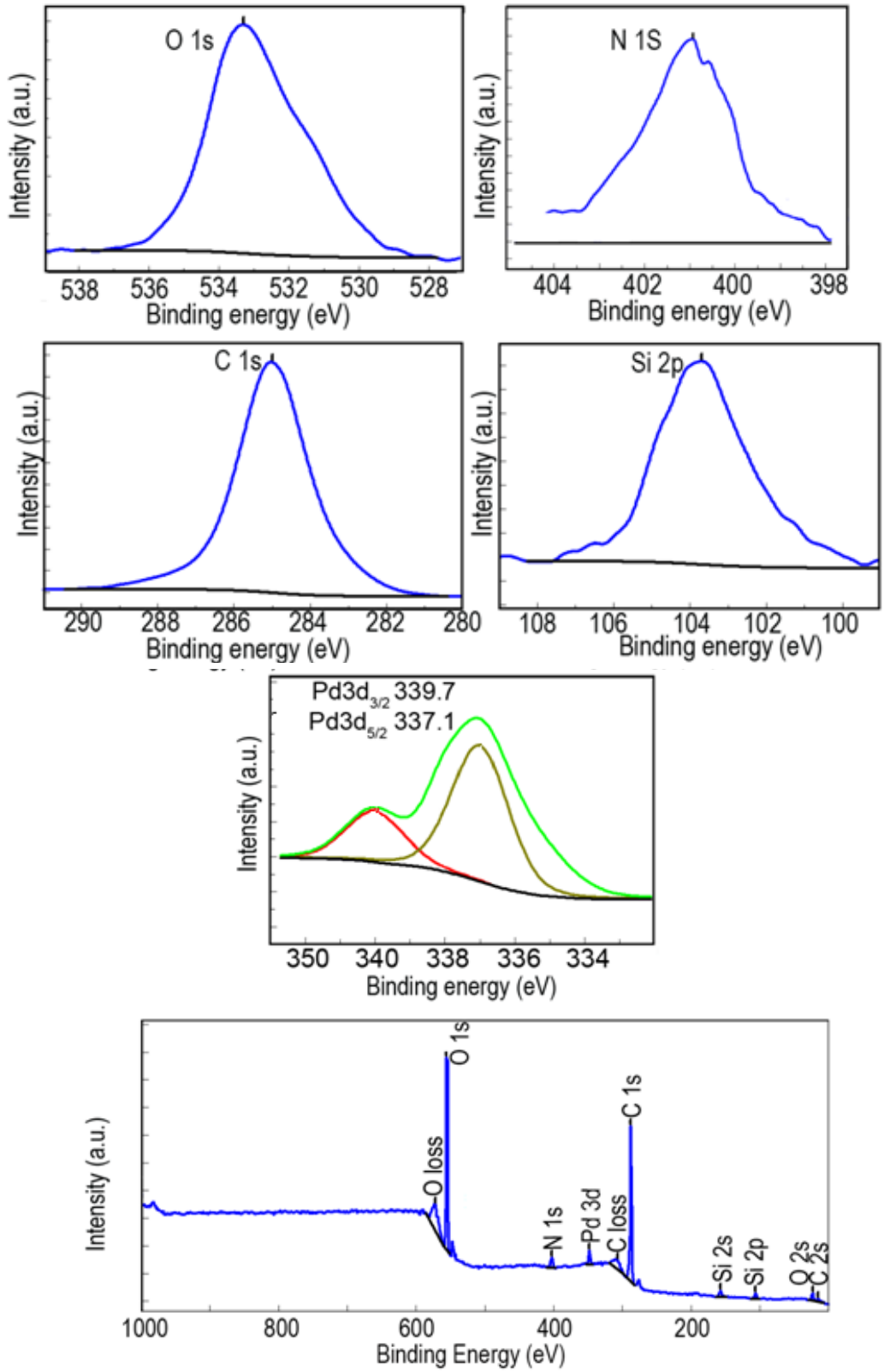

Fig. 8. XPS spectra of O 1s, N 1s, C 1s, Si 2p, Pd 3d and Pd@modified SBA-15.

Table 2. Optimization of reaction conditions, using different catalysts [a].

Entry	Catalyst (amount)	Solvent (reflux)	Time (min)	Yield[a] %
1	none	EtOH	400	7
2	NiO (5 mol%)	EtOH	350	27
3	$NaHSO_4$ (6 mol%)	EtOH	300	32
4	Ligand (5 mol%)	EtOH	200	35
5	SBA-15 (5 mol%)	EtOH	200	60
6	modified SBA-15 (8 mg)	EtOH	150	67
7	Pd@modified SBA-15 (4 mg)	EtOH	50	85
8	Pd@modified SBA-15 (6 mg)	EtOH	50	94
9	Pd@modified SBA-15 (8 mg)	EtOH	50	94
10	Pd@modified SBA-15 (8 mg)	H_2O	140	67
11	Pd@modified SBA-15 (8 mg)	DMF	130	73
12	Pd@modified SBA-15 (8 mg)	CH_3CN	80	80

[a] 4-Nitrobenzaldehyde (1 mmol), malononitrile (1 mmol) and 4-hydroxycoumarin (1 mmol)
[b] Isolated yield

shows the parallel channels (Fig. 4 c).

From the FT-IR spectra (Fig. 5), the SBA-15 spectrum displays a broad absorption band at 3439 cm^{-1} that is associated with the presence of silanol groups. A low-intensity band at 1632 cm^{-1} is attributed to the deformation modes of O-H bonds from adsorbed water. The Si-O-Si bond stretching vibrations with the bending vibrations are revealed at 1077 cm^{-1}, 801 cm^{-1}, and 455 cm^{-1}. The stretching vibrations of the Si-OH and Si-O-Si bonds appear as a weak band at 960 cm^{-1}. The peaks that are related to silica network of SBA-15 are observed with the same intensity in all the processes of functionalization. In the spectrum of chlorinated-SBA-15, the peaks at 3114 cm^{-1} and 1590 cm^{-1} are associated with the vibrations of C–H bonds in the propyl group. A peak at 709 cm^{-1} can be attributed to the C-Cl bonds. The results of the ^1H NMR spectrum of the ligand are approved by FT-IR spectrum. The FT-IR spectrum of ligand exhibits three sharp peaks at 1730, 1665 and 1610 cm^{-1} attributed to the C=O and C=C, respectively. Further, the absorption band at 3450 cm^{-1} is attributed to the NH stretching vibrations. By loading Pd, the intensity of the absorption band at 3450 cm^{-1} has diminished and slightly moved towards the lower frequency region. The absorption band at 1520 cm^{-1} has appeared due to ring >C=N stretching vibration. Based on the results, the complexion of Pd ions with modified SBA-15 has been approved.

The peaks of carbon, nitrogen, oxygen, silicon, and palladium become visible in the EDX spectra that confirmed the uniform distribution of ligand and palladium over SBA-15 (Fig. 6). The weight percentages of elements are calculated by EDX: C (21.97%), N (5.75%), O (46.90%), Si (20.80%), Pd (4.58%).

The TGA analysis shows that Pd@modified SBA-15 has higher weight loss than that of neat SBA-15 (Fig. 7). The weight loss was measured at about 28% up to 300 °C in two steps. The removal of physically absorbed water took place at the first step, and thermal decomposition of the organic functional group started above 300 °C. Consequently, the high decomposition temperature (above 300 °C) was the evidence of the high thermal stability of complex Pd/ligand.

The atomic concentration of catalyst and electronic state of the palladium has been characterized by X-Ray photoelectron spectroscopy (Fig. 8). N 1s, C 1s, and Pd 3d peaks are found on

Table 3. Synthesis of chromenes using Pd@modified SBA-15 (6 mg) under reflux conditions[a].

Entry	Aldehyde (R)	Product	Time (min)	Yield (%)	mp (°C) found
1	4-NO_2	4a	50	94	260-262
2	4-Br	4b	50	91	255-257
3	4-OCH_3	4c	90	79	242-244
4	H	4d	60	88	258-260
5	4-$(CH_3)_2CH$	4e	70	81	235-237
6	2-Me	4f	70	86	256-258
7	2,4-Cl	4g	50	92	255-257
8	3-OH	4h	90	80	262-264
9	4-Me	4i	90	84	261-263
10	2-OMe	4j	90	80	247-249

[a] Aromatic aldehydes (1 mmol), malononitrile (1 mmol) and 4-hydroxycoumarin (1 mmol)
[b] Isolated yield

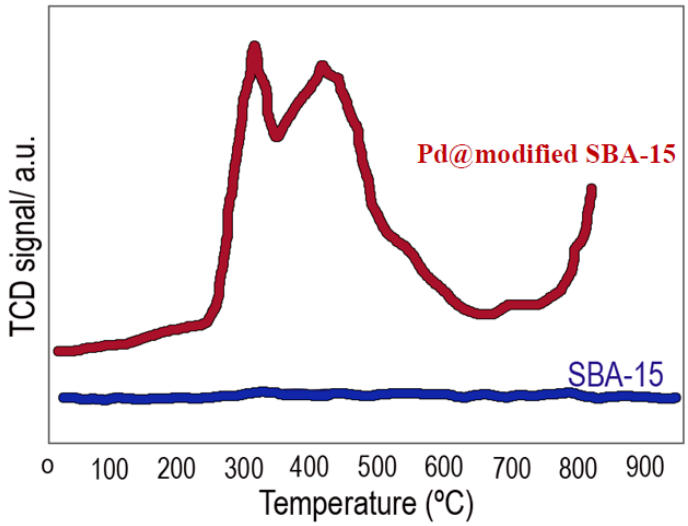

Fig. 9. NH_3-TPD spectra of SBA-15 and Pd@modified SBA-15.

the side of Si 2s, Si 2p, and O 1s peaks that approve the loading of ligand and metal on the SBA-15 surface. The N 1s spectrum of Pd@modified SBA-15 shows a peak at 401 eV due to σ*(N-H) resonance. Also, a shoulder is observed at 400 eV, which may be caused by π*(NHC=O). Amide π* resonances occur at very similar energies as the σ*(N–H) resonance. The intense and broad C 1s spectrum has exhibited a peak at 285 eV for C–Si, C–H*, σ*(C–C), and σ*(C–N) resonances [32]. The presence of the SiO_2 structure is confirmed by binding energies at 103 and 150 eV for Si 2s and Si 2p, respectively [33]. Binding energy of O 1s is 533.52 eV that could be assigned to Si-O, C-O, and C=O. Two distinct peaks at 337.1 and 339 eV have been observed in Pd 3d spectrum of Pd@modified

Table 4. Comparison of catalytic activity of Pd@modified SBA-15 with other reported catalysts.

Entry	Catalyst	Time (min)	Yield,[a] %	[Ref]
1	Et_3N	500	75	[15]
2	DBU	90	86	[18]
3	TEBA (triethylbenzylammonium chloride	240	88	[20]
4	[bmim]OH	80	85	[21]
5	Pd@modified SBA-15 (4 mg)	50	94	This work

[a] Isolated yield

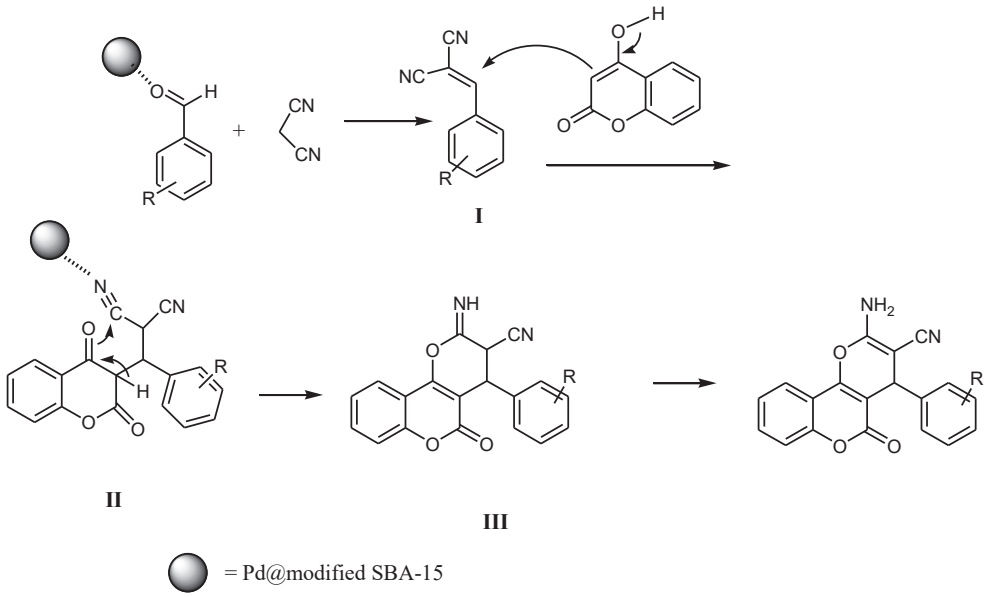

Scheme 3. Proposed mechanism for the synthesis of chromenes.

SBA-15 which is associated with 3d 5/2 and 3d 3/2, respectively. Atomic percentage concentrations of the Pd@modified SBA-15 are calculated by XPS: C (77.58), N (6.87), O (9.41), Si (5.42), Pd(0.15).

NH_3-TPD analysis has been used to calculate the surface acidity of the catalyst (Fig. 9). The TPD curve of initial SBA-15 exhibits no peaks that determined SBA-15 material has no acidity. The immobilization of Pd/Ligand complex leads to improve the acidity of catalyst as compared to initial SBA-15. The TPD curve of Pd@modified SBA-15 represents a sharp peak at 300 ˚C and a peak at around 450 ˚C that are correlated with weak and medium acid sites, respectively. Also, there is a shoulder peak at ca. 550 ˚C that is attributed to strong acid sites. Indeed, there are some weak, medium, and strong acid sites in the Pd@modified SBA-15 that make it such an effective catalyst.

We used the reaction of malononitrile, 4-nitrobenzaldehyde, and 4-hydroxycoumarin as a model procedure and carried it out in the presence of NiO, $NaHSO_4$, Ligand, SBA-15, modified SBA-15, and Pd@modified SBA-15. The results are summarized in Table 2. We found that the reaction gave very useful results in the presence of Pd@modified SBA-15 (6 mg for a 1 mmole scale reaction) under reflux conditions. Further to this, we also reacted malononitrile and 4-hydroxycoumarin with other aromatic aldehydes and found uniformly good results (Table 3). Yields were slightly higher for aldehydes substituted with electron-withdrawing groups.

The reusability of our nanocatalyst was examined for the model reaction, and it was found that product yields lessened only to a very small extent on each reuse (run 1, 94%; run 2, 94%; run 3, 93%; run 4, 93%; run 5, 92%; run 6, 92%).

To compare the efficiency of Pd@modified SBA-15 with the reported catalysts for the synthesis of chromenes, the results are tabulated in Table 4. Our study has some advantages in comparison with other mentioned studies, including high yields of synthetic compounds, reasonable reaction times and easy catalyst recovery.

Scheme 3 shows a plausible mechanism for this process in the presence of Pd@modified SBA-15. We propose that the reaction occurs via a condensation between malononitrile and aldehyde, to form intermediate I on the active sites of the Pd@modified SBA-15. Then, 4-hydroxycoumarin adds to intermediate I to give intermediate II The intermediate III is subsequently formed by an intra-molecular cyclization reaction Tautomerization will provide the final product. In this mechanism the surface atoms of Pd@modified SBA-15 activate the C=O and C≡N groups for better reaction with nucleophiles.

CONCLUSIONS

In conclusion, we have reported an efficient procedure for the synthesis of chromenes through a three-component reaction involving aromatic aldehydes, malononitrile and 4-hydroxycoumarin. We found that the reaction gave very useful results in the presence of Pd@modified SBA-15 (6 mg for a 1 mmol scale reaction) under reflux conditions. Further to this, we also reacted malononitrile and 4-hydroxycoumarin with other aromatic aldehydes and found uniformly good results. Yields were slightly higher for aldehydes substituted with electron-withdrawing groups.

The catalyst has been characterized by XRD, FE-SEM, TEM, EDX, XPS, FT-IR, N_2 adsorption analysis, TPD, and TGA-DTA. The advantages of this method include very good yields, the excellent reusability of the catalyst, low catalyst loading, and easy separation of products, with no recrystallization required.

CONFLICT OF INTEREST

The authors declare no conflict of interest.

REFERENCES

1 M. S. L. Kumar, J. Singh, S. K. Manna, S. Maji, R. Konwar, G. Panda, Diversity oriented synthesis of chromene-xanthene hybrids as anti-breast cancer agents, Bioorg. Med. Chem. Lett., 28, 778-782 (2018). https://doi.org/10.1016/j.bmcl.2017.12.065

2 U. S. Rai, A. M. Isloor, P. Shetty, A. M. Vijesh, N. Prabhu, S. Isloor, M. Thiageeswaran, H. K. Fun, Novel chromeno [2, 3-b]-pyrimidine derivatives as potential anti-microbial agents, Eur. J. Med. Chem., 45, 2695-2699 (2010). https://doi.org/10.1016/j.ejmech.2010.02.040

3 I. V. Ilyina, V. V. Zarubaev, I. N. Lavrentieva, A. A. Shtro, I. L. Esaulkova, D. V. Korchagina, S. S. Borisevich, K. P. Volcho, N. F. Salakhutdinov, Highly potent activity of isopulegol-derived substituted octahydro-2H-chromen-4-ols against influenza A and B viruses, Bioorg. Med. Chem. Lett., 28, 2061-2067 (2018). https://doi.org/10.1016/j.bmcl.2018.04.057

4 S. T. Chung, W. H. Huang, C. K. Huang, F. C. Liu, R. Y. Huang, C. C. Wu, A. R. Lee, Synthesis and anti-inflammatory activities of 4H-chromene and chromeno[2,3-b]pyridine derivatives, Res. Chem. Intermed., 42, 1195-1215 (2016). https://doi.org/10.1007/s11164-015-2081-7

5 S. Li, H. Xu, S. Cui, F. Wu, Y. Zhang, M. B. Su, Y. Gong, S. Qiu, H. Li, Discovery and rational design of natural-product-derived 2-phenyl-3,4-dihydro-2h-benzo[f] chromen-3-amine analogs as novel and potent dipeptidyl peptidase 4 (dpp-4) inhibitors for the treatment of type 2 diabetes, J. Med. Chem., 59, 6772-6790 (2016). https://doi.org/10.1021/acs.jmedchem.6b00505

6 M. I. Fernández-Bachiller, C. Pérez, L. Monjas, J. Rademann, M. I. Rodríguez-Franco, New tacrine-4-oxo-4h-chromene hybrids as multifunctional agents for the treatment of alzheimer's disease, with cholinergic, antioxidant, and β-amyloid-reducing properties, J. Med. Chem., 55, 1303-1317 (2012). https://doi.org/10.1021/jm201460y

7 N. Thomas and S. M. Zachariah, Pharmacological activities of chromene derivatives: an overview, Asian J. Pharm. Clin. Res., 6, 11-15 (2013).

8 A. Shokri, Degradation of terphetalic acid from petrochemicalwastewaterbyozonationando3/znoprocesses in semi batch reactor, Arch Hyg Sci., 6, 348-355 (2017). https://doi.org/10.29252/ArchHygSci.6.4.348

9 A. Shokri, Employing sono-fenton process for degradation of 2-nitrophenol in aqueous environment using box-behnken design method and kinetic study, Russ. J. Phys. Chem., 93, 243-249 (2019). https://doi.org/10.1134/S003602441902002X

10 M. Saghi, A. Shokri, A. Arastehnodeh, M. Khazaeinejad, A. Nozari, The photo degradation of methyl red in aqueous solutions by α-Fe2O3/SiO2 nano photocatalyst, J. Nanoanalysis.,5, 163-170 (2018).

11 A. Shokri, Using Mn based on lightweight expanded clay aggregate (LECA) as an original catalyst for the removal of NO2 pollutant in aqueous environment, Surf. Interfaces, 21, 100705-100710 (2020). https://doi.org/10.1016/j.surfin.2020.100705

12 A. Shokri, Using NiFe2O4 as a nano photocatalyst for degradation of polyvinyl alcohol in synthetic wastewater, Environmental Challenges, 5, 100332-100339 (2021). https://doi.org/10.1016/j.envc.2021.100332

13 F. Yang, H. Wang, L. Jiang, H. Yue, H. Zhang, Z. Wang, L. Wang, A green and one-pot synthesis of benzo [g] chromene derivatives through a multi-component reaction catalyzed by lipase, RSC. Adv., 5, 5213-5216 (2015).

https://doi.org/10.1039/C4RA13272F
14 R. Ghahremanzadeh, T. Amanpour, A. Bazgir, An efficient, three-component synthesis of spiro[benzo[g]chromene-4,3′-indoline]-3-carbonitrile and spiro[indoline-3,5′-pyrano[2,3-d] pyrimidine]-6′-carbonitrile derivatives, J. Heterocyclic Chem., 46, 1266-1270 (2009). https://doi.org/10.1002/jhet.240
15 A. Shaabani, R. Ghadari, S. Ghasemi, M. Pedarpour, A. H. Rezayan, A. Sarvary, S. W. Ng, Novel one-pot three- and pseudo-five-component reactions: synthesis of functionalized benzo[g]- and dihydropyrano[2,3-g] chromene derivatives, J. Comb. Chem., 11, 956-959 (2009). https://doi.org/10.1021/cc900101w
16 J. Khalafy, S. Ilkhanizadeh, M. Ranjbar, A green, organometallic catalyzed synthesis of a series of novel functionalized 4-aroyl-4H-benzo[g] chromenes through one-pot, three component reaction, J. Heterocyclic Chem., 55, 951-956 (2018). https://doi.org/10.1002/jhet.3124
17 F. Khorami, H. R. Shaterian, Preparation of 2-amino-3-cyano-4-aryl-5, 10-dioxo-5, 10-dihydro-4 H-benzo [g] chromene and hydroxyl naphthalene-1, 4-dione derivatives, Res. Chem. Intermed., 41, 3171-3191 (2015). https://doi.org/10.1007/s11164-013-1423-6
18 J. M. Khurana, B. Nand, P. Saluja, DBU: a highly efficient catalyst for one-pot synthesis of substituted 3,4-dihydropyrano[3,2-c]chromenes, dihydropyrano[4,3-b]pyranes, 2-amino-4H-benzo[h] chromenes and 2-amino-4H benzo[g]chromenes in aqueous medium, Tetrahedron, 66, 5637-5641 (2010). https://doi.org/10.1016/j.tet.2010.05.082
19 M. Perumal, P. Sengodu, S. Venkatesan, R. Srinivasan, M. Paramsivam, Environmentally benign copper triflate-mediated multicomponent one-pot synthesis of novel benzo[g]chromenes possess potent anticancer activity, Chem. Select., 2, 5068-5072 (2017). https://doi.org/10.1002/slct.201700170
20 C. Yao, C. Yu, T. Li, S. Tu, An efficient synthesis of 4h-benzo[g]chromene-5,10-dione derivatives through triethylbenzylammonium chloride catalyzed multicomponent reaction under solvent-free conditions ,Chin. J. Chem., 27, 1989-1994 (2009). https://doi.org/10.1002/cjoc.200990334
21 Y. Yu, H. Guo, X. Li, An improved procedure for the three-component synthesis of benzo[g] chromene derivatives using basic ionic liquid, J. Heterocyclic Chem., 48, 1264-1268 (2011). https://doi.org/10.1002/jhet.747
22 K. Gong, H. L. Wang, J. Luo, Z. L. Liu, One-pot synthesis of polyfunctionalized pyrans catalyzed by basic ionic liquid in aqueous media, J. Heterocyclic Chem., 46, 1145-1150 (2009). https://doi.org/10.1002/jhet.193
23 H. Kiyani, M. Tazari, Aqua one-pot, three-component synthesis of dihydropyrano[3,2-c]chromenes and amino-benzochromenes catalyzed by sodium malonate, Res. Chem. Intermed., 43, 6639-6650 (2017). https://doi.org/10.1007/s11164-017-3011-7
24 F. Schueth, W. Schmidt, Microporous and mesoporous materials. Adv. Eng. Mater. 4, 269-279 (2002). https://doi.org/10.1002/1527-2648(20020503)4:5<269::AID-ADEM269>3.0.CO;2-7
25 F. Tang, L. Li, D. Chen, Mesoporous silica nanoparticles: synthesis, biocompatibility and drug delivery. Adv. Mater. 24, 1504-1534 (2012). https://doi.org/10.1002/adma.201104763
26 H. Atashin, R. Malakooti, Magnetic iron oxide nanoparticles embedded in SBA-15 silica wall as a green and recoverable catalyst for the oxidation of alcohols and sulfides, J. Saudi Chem. Soc. 21, S17-S24 (2017). https://doi.org/10.1016/j.jscs.2013.09.007
27 J. Li, L. Wang, T. Qi, Y. Zhou, C. Liu, J. Chu, Y. Zhang, Different N-containing functional groups modified mesoporous adsorbents for Cr (VI) sequestration: Synthesis, characterization and comparison. Microporous Mesoporous Mater. 110, 442-450 (2008). https://doi.org/10.1016/j.micromeso.2007.06.033
28 H. G. Hosseini, S. Rostamnia, Post-synthetically modified SBA-15 with NH2-coordinately immobilized iron-oxine: SBA-15/NH2-FeQ3 as a Fenton-like hybrid catalyst for the selective oxidation of organic sulfides. New J. Chem. 42, 619-627 (2018). https://doi.org/10.1039/C7NJ02742G
29 J. Safaei-Ghomi, A. Bakhtiari, Tungsten anchored onto functionalized SBA-15: an efficient catalyst for diastereoselective synthesis of 2-azapyrrolizidine alkaloid scaffolds. RSC adv. 9, 19662-19674 (2019). https://doi.org/10.1039/C9RA02825K
30 M. Vengatesan, S. Devaraju, K. Dinakaran, M. Alagar, SBA-15 filled polybenzoxazine nanocomposites for low-k dielectric applications. J. Mater. Chem. 22 (2012) 7559-7566. https://doi.org/10.1039/c2jm16566j
31 K. Bendahou, L. Cherif, S. Siffert, H. Tidahy, H. Benaissa, A. Aboukais, The effect of the use of lanthanum-doped mesoporous SBA-15 on the performance of Pt/SBA-15 and Pd/SBA-15 catalysts for total oxidation of toluene. Appl. Catal., A. 351, 82-87 (2008). https://doi.org/10.1016/j.apcata.2008.09.001
32 N. Graf, E. Yegen, T. Gross, A. Lippitz, W. Weigel, S. Krakert, A. Terfort, W. E. Unger, XPS and NEXAFS studies of aliphatic and aromatic amine species on functionalized surfaces. Surf. Sci. 603, 2849-2860 (2009). https://doi.org/10.1016/j.susc.2009.07.029
33 C. Hess, G. Tzolova-Müller, R. Herbert, The influence of water on the dispersion of vanadia supported on silica SBA-15: a combined XPS and Raman study, J. Phys. Chem. C.111, 9471-9479 (2007). https://doi.org/10.1021/jp0713920